Ocean Model Working Group Meeting, Feb. 8-10, 2023

The SubAntarctic Zone - Water Mass Formation and climate change

R. Justin Small, NCAR
Daniel Whitt, NASA Ames,
Ivana Cerovečki, Matthew Mazloff, Scripps
Gaopeng Xu, Ping Chang
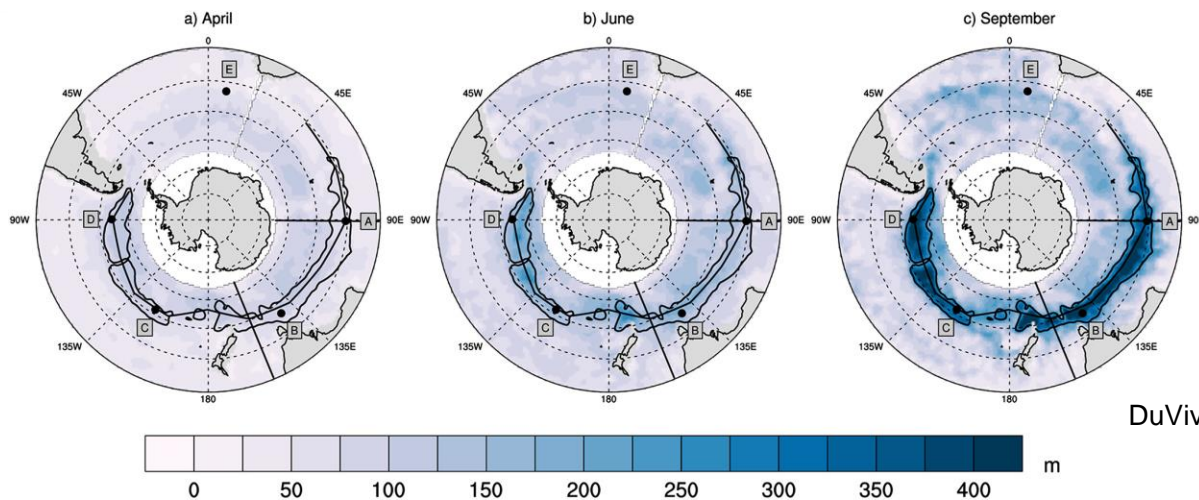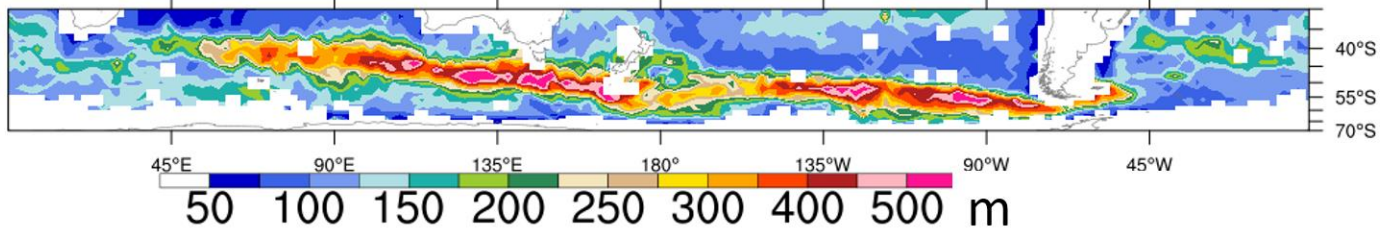*Department of Oceanography, Texas A&M*

Spiralling nature of SubAntarctic deep Mixed Layer Depth (MLD)

Note: the ACC and ocean fronts also spiral

Austral winter MLD: Argo 2000-2017 (mostly post 2004)

Chang et al. 2020, JAMES

a) April   b) June   c) September

DuVivier et al. 2019, JGR Oceans

Argo observations
T/S from gridded 1deg. Product (Roemmich and Gilson 2009)
Mixed layer depth from Whitt, Nicholson, Carranza 2019, JGR Oceans
(Uses maximum buoyancy gradient method: 2deg. grid)

NCAR
UCAR

Outline

- 1) Using Water Mass Formation ideas to understand SubAntarctic Modewater formation and variability.
  - Water Mass Formation Maps
  - Water Mass Formation in T/S space
- 2) Climate change of upper ocean temperature in the SubAntarctic Zone.
  - High-resolution vs low-resolution climate models
  - Ocean heat budget approach
  - Role of oceanic advection and mixing vs surface warming

NCAR
UCAR

Preview

- Water Mass Formation (WMF)
  - Spatial maps of WMF give detailed information about where deep MLD and SAMW form
  - WMF in T/S space allows us to understand the volume census and storage in SubAntarctic Zone
  - The WMF can be used quantitatively in volume budgets to identify processes of formation, destruction, & movement of water masses

- Reduced SST and upper ocean heat content warming under climate change in SubAntarctic zone in CESM-HR
  - Combination of the effects of ocean advection and also vertical mixing
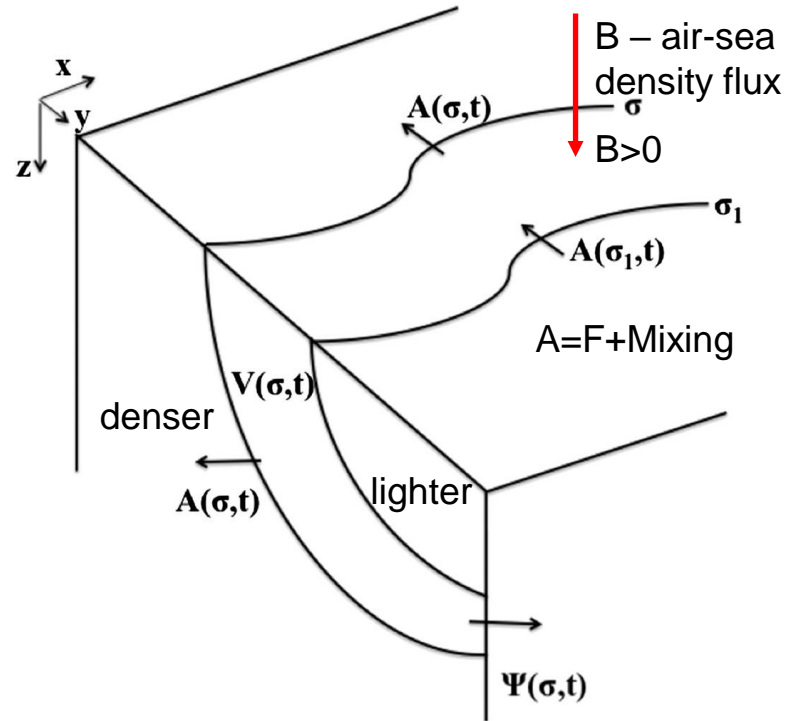
Water Mass Formation background

Surface Water Mass Transformation F

$$F(\sigma) = \frac{1}{\Delta\sigma} \iint_{Area} B \, \Pi(\sigma_1, \sigma) dArea$$

Air-Sea density flux

Surface Water Mass Formation M

$$M = -\Delta\sigma \frac{\partial F}{\partial \sigma}$$

B – air-sea density flux

B>0

A=F+Mixing

denser

lighter

From Cerovecki and Mazloff 2016, J. Phys. Oceanogr, Nishikawa et al. 2013, JGRO. Schematic of volume budget for the control volume $V(\sigma, t)$, bounded by the intersection with the sea surface, the two isopycnal surfaces σ_1 and σ, and by the open boundary (set at 30°S in our analysis). The arrows labeled $A(\sigma_1, t)$ and $A(\sigma, t)$ are diapycnal volume fluxes, and $\psi(\sigma, t)$ is the volume flux out of $V(\sigma)$. The transformation rate $A(\sigma, t)$ is the sum of interior $[\partial D(\sigma)/\partial\sigma]$ and surface $[F(\sigma)]$ components.

- Walin (1982), Tziperman (1986), Speer and Tziperman (1992), Nurser et al. 1999, Marshall et al. 1999, Large and Nurser 2001, Nishikawa et al. 2013, etc., reviewed by Groeskamp et al. 2019

NCAR
UCAR

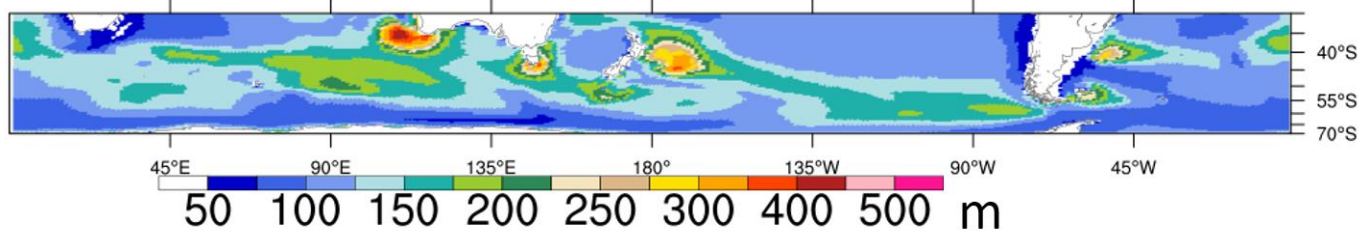# High Resolution CESM simulations

- High-resolution CESM1
  - CAM5 and POP2, CICE4, CLM4
  - HR (0.1deg. Ocean & Ice, 0.25deg atmosphere & land)
  - LR (1deg. Ocean & Ice, 1deg. Or 0.25deg. Atmosphere & land)
- "ASD" run
  - CESM1.1 Year 2000 conditions
  - 100 year control
  - Run on Yellowstone (Small et al. 2014)
- iHESP simulations
  - CESM1.3 (Meehl et al. 2019)
  - Sunway HPC (Zhang et al. 2019)
  - 1850 PI CTL (Chang et al. 2020)
  - Transient run branched from 1850 PI CTL (Chang et al. 2020)
  - 1850-2005 historical forcing, then 2006-2100 RCP8.5
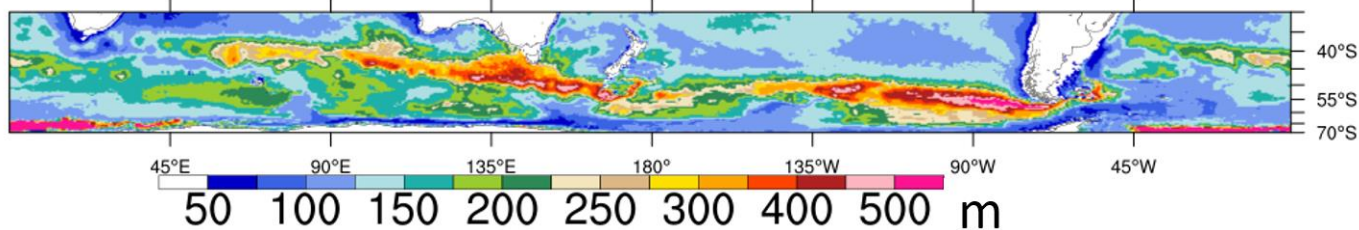
Motivation (1): MLD in Climate Models

Austral winter MLD: Argo 2000-2017 (mostly post 2004)
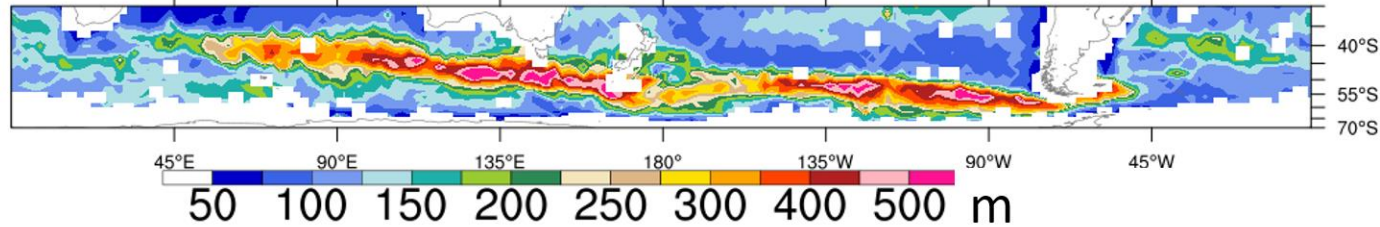
Austral winter MLD: IHESP Low-Res 2006-2020


LR has very shallow mixed layers. Deepest mixed layers are in the wrong location.
Excessive shallow bias in Pacific Ocean.

Austral winter MLD: IHESP High-Res 2006-2020

HR has deep mixed layers in the correct location.
Shallow bias in Indian Ocean.

DuVivier et al. 2018 (JGR-O), Small et al. 2021 (Cli. Dyn.) found that the ocean mean geostrophic circulation and the salinity stratification was important in determining MLD spatial distribution.
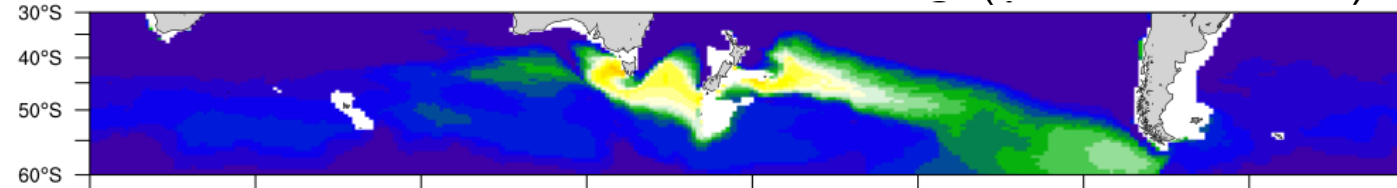
NCAR
UCAR

Motivation (2): SubAntarctic Modewater (SAMW) thickness in Climate Models
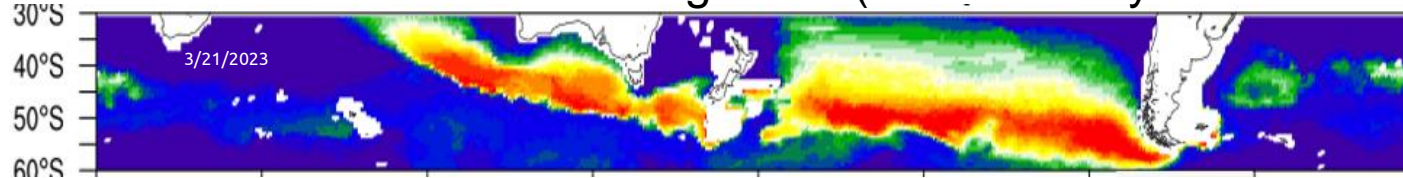
SAMW Thickness: Argo 2005-2009

SAMW Thickness: CESM Low-Res (Small et al. 2014)

SAMW Thickness: CESM High-Res (iHESP CTL years 320-329)
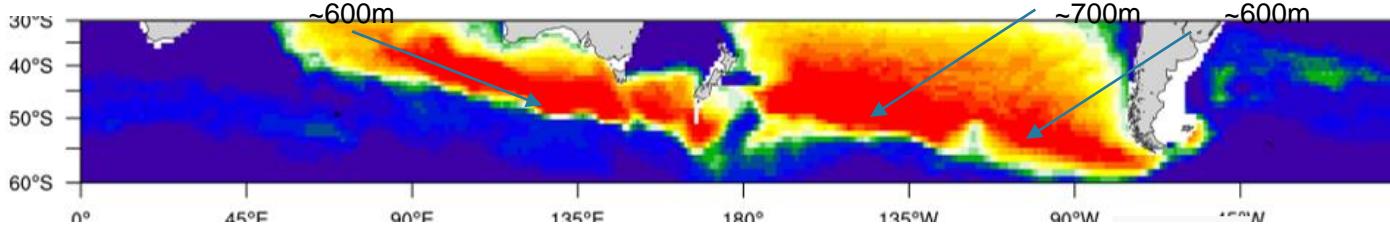
SAMW (McCartney 1977, 1982), Hanawa and Talley (2000), Cerovecki et al. (2013)

SAMW defined by potential densities between *1026.5* and 1027.1kgm^{-3}, and PV less than *50**10^{-12}m^{-1}s^{-1}

High-resolution CESM produces Modewater in correct location as a consequence of the deep MLD in previous slide. Low-resolution is deficient in this regard.
This is a justification to use high-resolution CESM to study the Water Mass Formation (next).

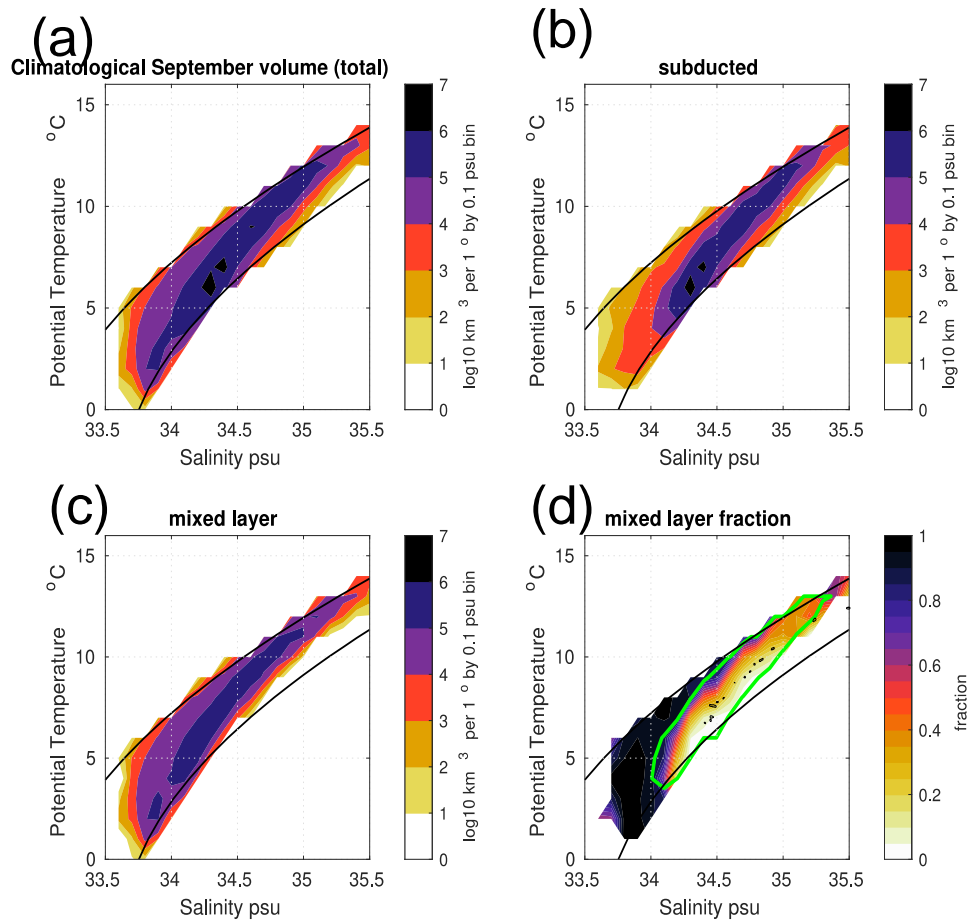# Motivation (3): Volume census in Argo (courtesy Dan Whitt)

Figure. Volumetric histograms of climatological September SAMW disaggregated into T-S bins and separated into mixed-layer and subducted (below-mixed-layer) pools. Black lines bound the potential density range 1026.6-1027.1 kg/m3. (a) is the total volume, (b) is the subducted volume, (c) is the volume in the mixed layer, and (d) is the ratio mixed-layer over subducted volume. The green contour in (d) indicates subducted volume < 104 km3 per 1 deg/0.1 psu bin. Overlaid in (d) are the T/S properties of deep mixed layers identified by McCartney 1977 (his Fig 7) as examples of SAMW formation (small black circles).

Motivation (4): SST change from 1950-1980 to 2070-2100

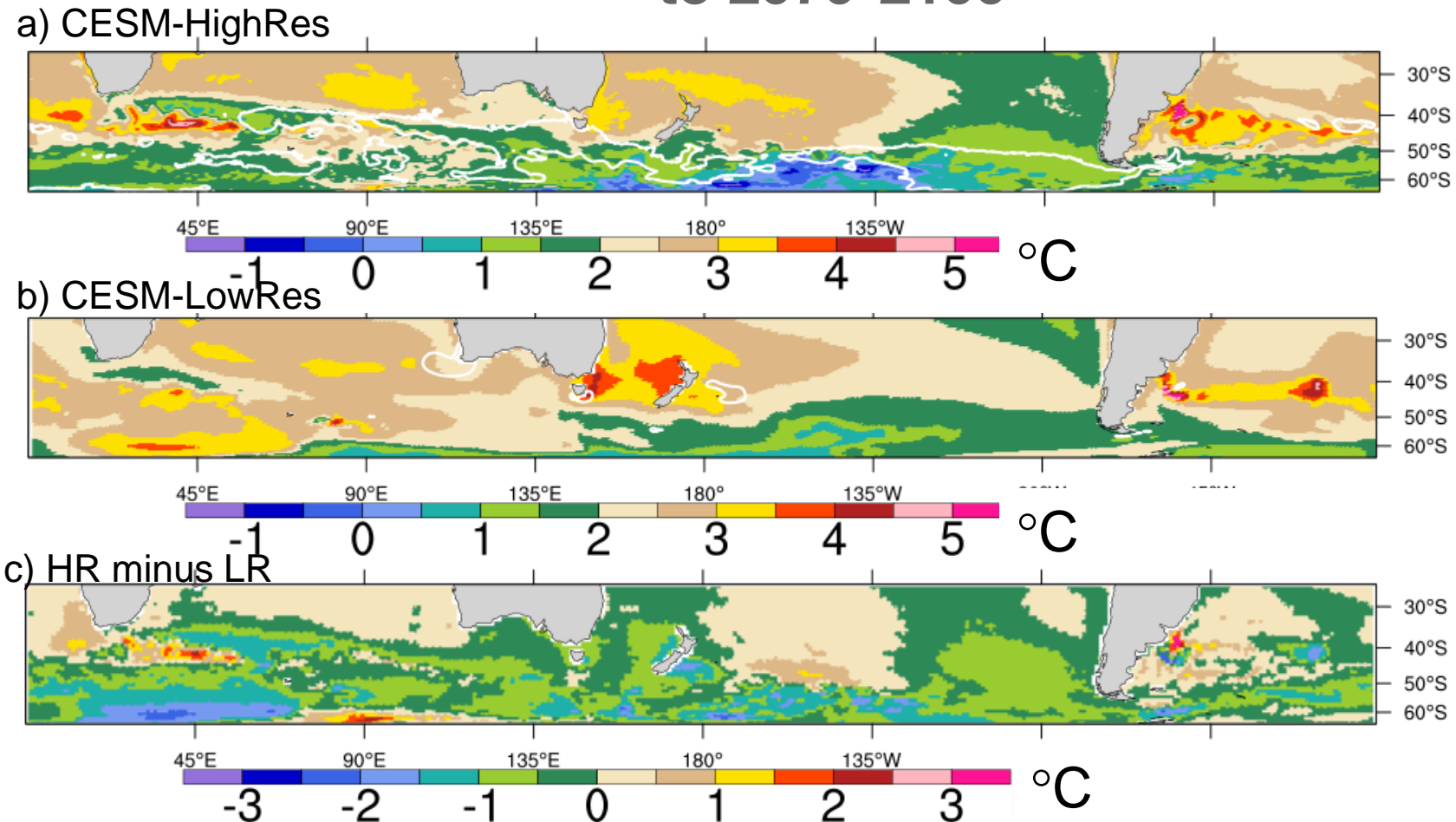a) CESM-HighRes

b) CESM-LowRes

c) HR minus LR

Fig 3. SST change from 1950-1980 to 2070-2100 for Top: CESM-HR and Middle: CESM-LR. Overlaid is the 125m MLD contour (annual mean). Bottom: the difference HR minus LR. Note that CESM-HR has generally less warming than CESM-LR. Some of this may be related to MLD, but other factors like sea-ice change may play a role.

Water Mass Formation maps to interpret SubAntarctic Modewater spatial distribution

- Water Mass Formation maps – Brambilla et al. (2008), Maze et al. (2009), Cerovecki et al. (2013)
- Volume budget in geographical space (Cerovecki et al. 2016)

- Here we present WMF maps for the SubAntarctic and note that the deep mixing band coincides with the Water Mass Formation region
  - Note also role of surface heat flux vs freshwater flux

The WMT and WMF can also be displayed in map form, following Brambilla et al. 2008, Maze et al. 2009, where the WMT map G averaged over a year is defined by
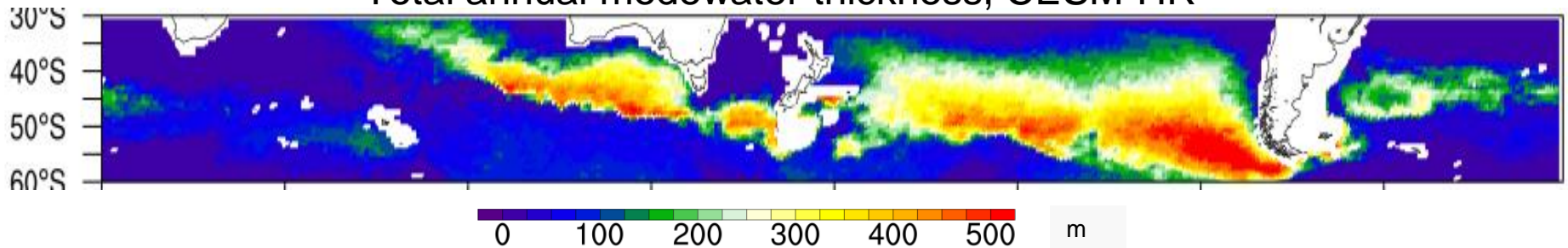
$$G\left(\sigma_1 + \frac{\Delta\sigma}{2}, x, y\right) = \frac{1}{365\Delta\sigma} \sum_{n=1}^{n=365} B(x,y,n) dx dy \ \Pi(\sigma_1, \sigma_2)$$

densification. A Water Mass Formation map was defined as the difference between these two consecutive maps (Maze et al. 2009):
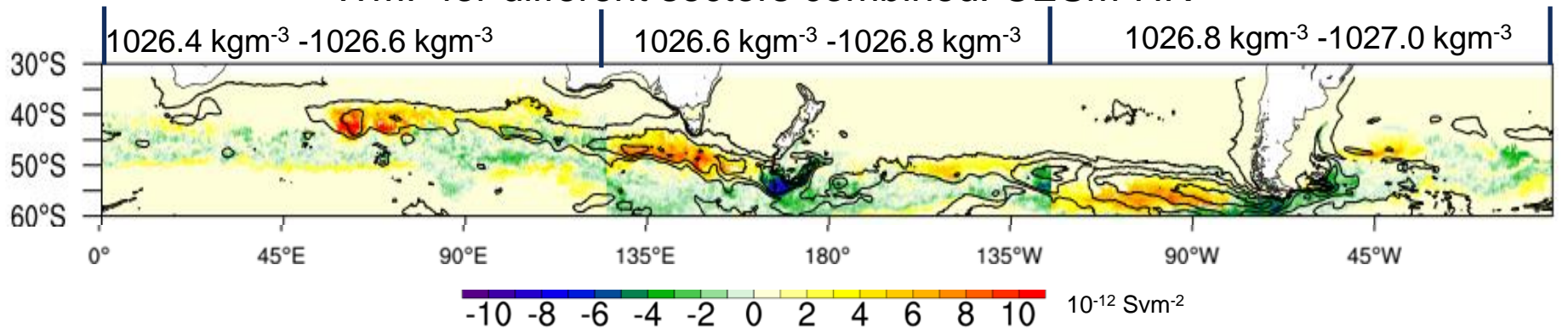
$$G\left(\sigma_1 - \frac{\Delta\sigma}{2}, x, y\right) - G\left(\sigma_1 + \frac{\Delta\sigma}{2}, x, y\right)$$

Water Mass Formation maps

Total annual modewater thickness, CESM-HR

WMF for different sectors combined: CESM-HR

1026.4 kgm^{-3} -1026.6 kgm^{-3} 1026.6 kgm^{-3} -1026.8 kgm^{-3} 1026.8 kgm^{-3} -1027.0 kgm^{-3}


10^{-12} Svm^{-2}

Note how the large positive Water Mass Formation (colors, lower panel) occurs in regions of deep MLD (contours) and is the formation region for SAMW (top panel).

Figure: Top panel shows the annual-mean SAMW thickness from CESM-HR, using a definition of PV < 5e-11m^{-1}s^{-1}, and for potential density (PD) range 1026.5kgm^{-3}<PD<1027.1 kgm^{-3}. The bottom panel shows Water Mass Formation maps for 3 ocean sectors combined into one: WMF for PD between 1026.4 kgm^{-3} and 1026.6 kgm^{-3} for 0°-125° E, between 1026.6 kgm^{-3} and 1026.8 kgm^{-3} for 125° E to 125° W, and between 1026.8 kgm^{-3} and 1027 kgm^{-3} for 125° W to 0°. This method of combining different sectors allows for choice of the appropriate SAMW densities for each basin. Overlaid is the July-August –September average mixed layer depth from Argo (Whitt et al. 2019, JGR(O)), contours at 100m, 200m, 300m, 400m, 500m.

WMF map *1e12 Sv_m2: Total:44.0 Sv
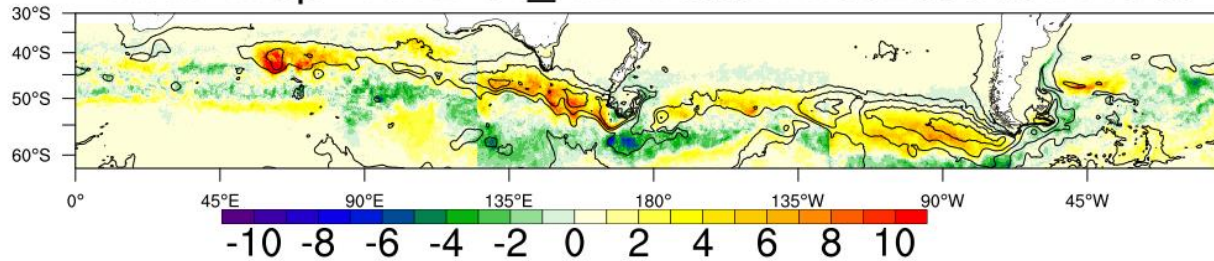
WMF map *1e12 Sv_m2: Total:38.6 Sv
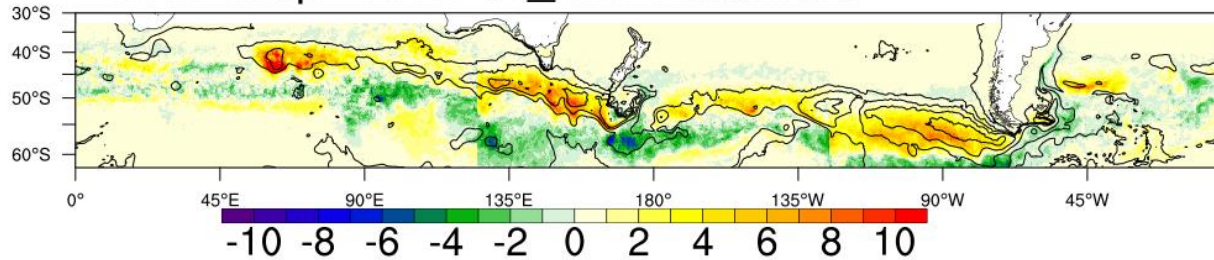
As previous panel, annual mean, but now lower panel shows the surface heat-flux-only contribution, which is dominant.

Water Mass Formation ideas to understand SubAntarctic Modewater distribution in T/S space.

- Relating WMF to classic T/S distributions and Mode Water Classifications.

- Speer and Tziperman 1992, Speer 1993, Hieronymous et al. 2014, Evans et al. 2014, 2018, Groeskamp et al. 2014, Ben Johnson 2020.

$$F\left(T_1 + \frac{\Delta T}{2}, S_1 + \frac{\Delta S}{2}\right) = \frac{1}{\Delta T \Delta S} \iiint_A B \ \Pi(T_1, T_2) \Pi(S_1, S_2) dA$$

- Eventual aim is to quantitatively relate the WMF in T/S space with the volume census and the storage rate.

- Acknowledging motivation from Ben Johnson for this topic!

# Water Mass Formation in T/S space + Volume Census
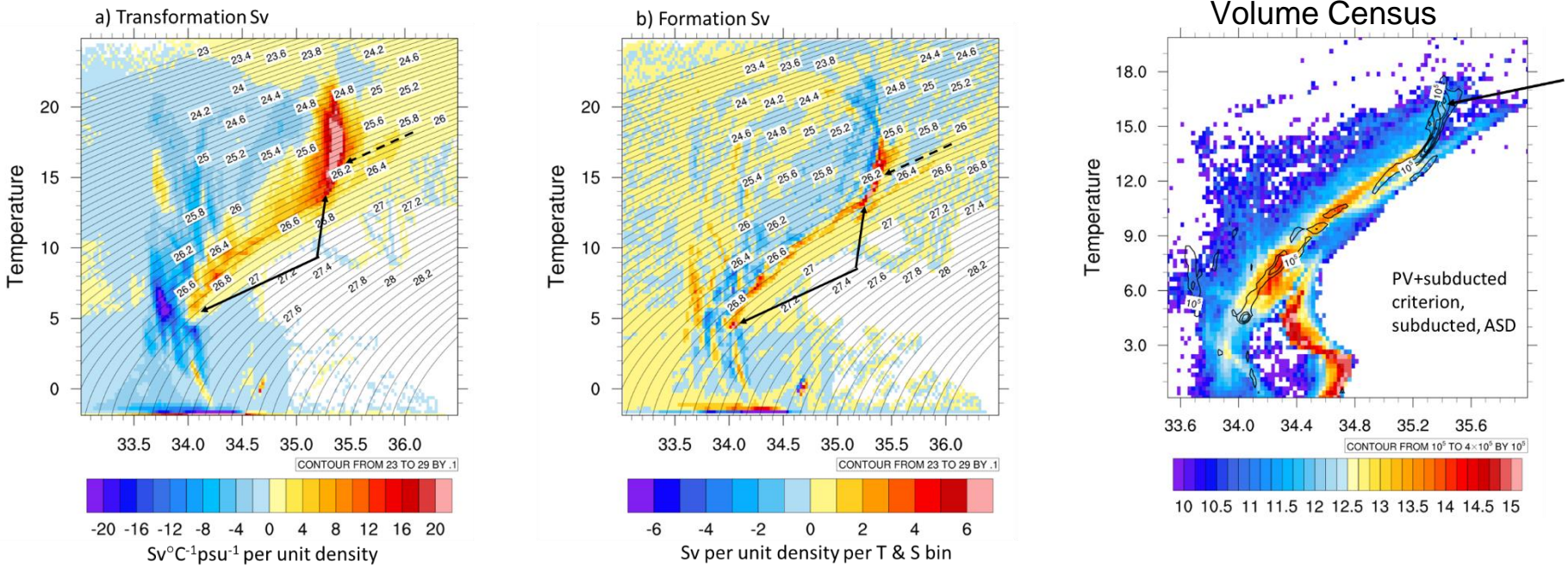
Left and middle. a) Water Mass Transformation and b) Formation in Temperature-Salinity space for the Southern Ocean. The arrows point to key transformation and formation features
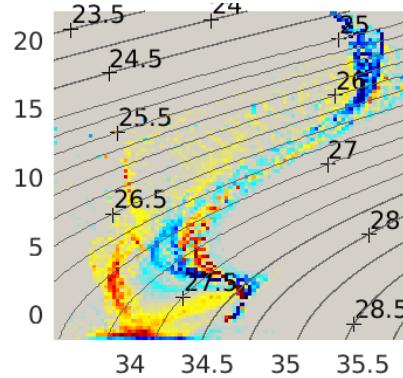
Right. Showing low PV subducted water but with contours of WMF left overlaid. Note that the large WMF generally overlies regions of large census, i.e. the SAMW.

Volume budget in T/S space from ECCO (courtesy of Ivana Cerovecki)
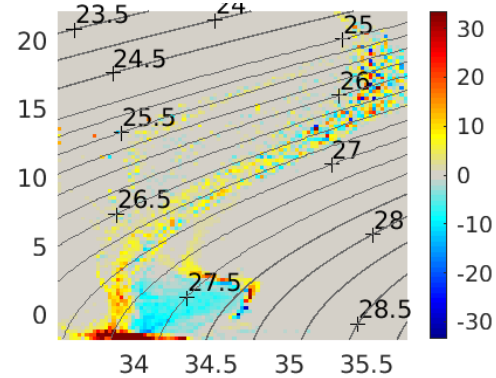
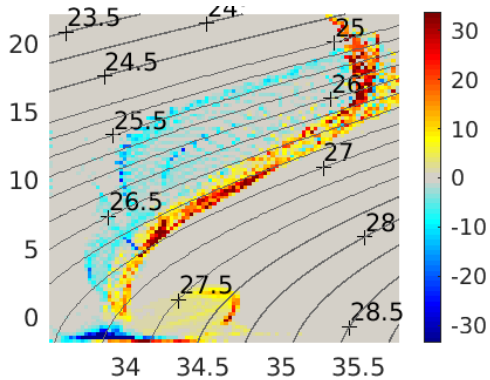

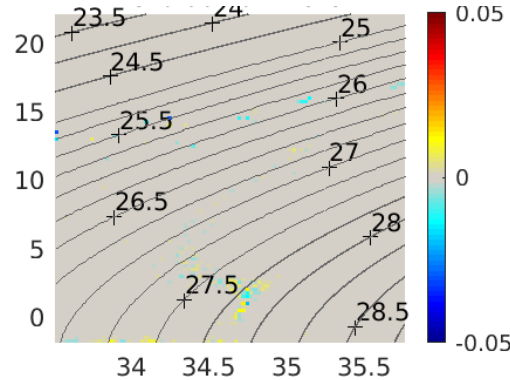Volume Tendency=Storage
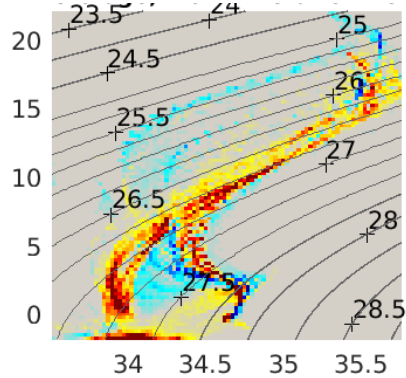
Tendency due to Advection

Tendency due to interior diapycnal mixing

Surface Water Mass Formation

Residual

Results are shown for month of September, peak formation period.

ECCO V4r3 state estimate, based on MIT GCM with grid of nominal resolution of 1° in space (Wunsch and Heimbach 2007, Piecuch 2017, Fukumori et al. 2017, Forget et al. 2015).
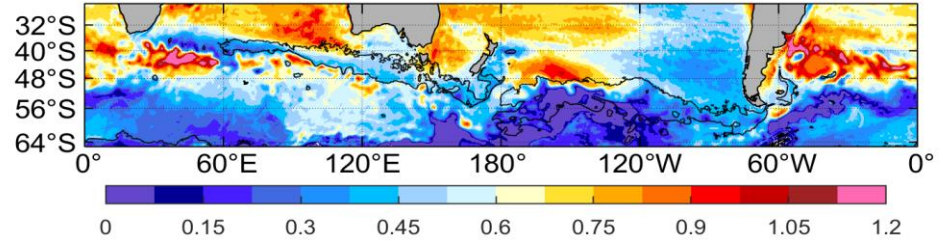
NCAR
UCAR

Climate change of SST

- Bilgen and Kirtman (2020) noted much reduced warming of Southern Ocean SST under climate change in high-resolution climate model under historical period,
  - Impact of ocean model resolution on understanding the delayed warming of the Southern Ocean, Env. Res. Letts., DOI 10.1088/1748-9326/abbc3e)
- What about climate change to 2100?
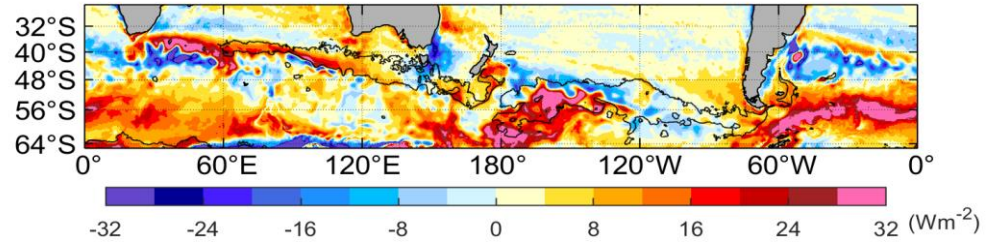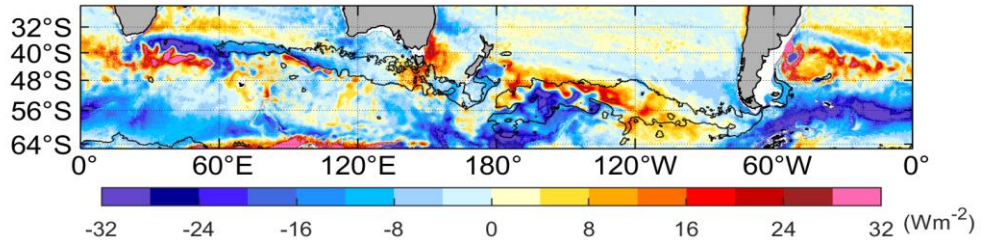 - Use IhesP high resolution "DECK" experiments

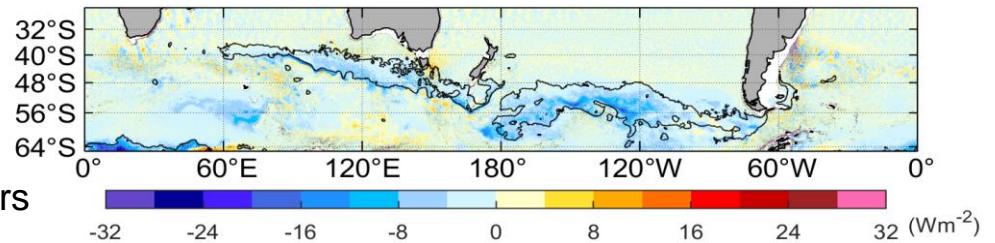NCAR
UCAR

HR

2000-2100, upper 200 m

Temp changes

$$\underbrace{\bar{T}(t) - \bar{T}(t_0)}_{\text{Temp. Change}} = \underbrace{-\int_{t_0}^{t} \left(\overline{u\frac{\partial T}{\partial x}} + \overline{v\frac{\partial T}{\partial y}} \right) dt - \int_{t_0}^{t} \overline{w\frac{\partial T}{\partial z}} dt}_{\text{Advection}}$$

$$\underbrace{+ \int_{t_0}^{t} \frac{1}{c_P \rho_0} (Q_{net} - SW|_{z=-h}) dt}_{\text{Net Atmos. Heating}} + \underbrace{R}_{\text{Mixing}},$$

Qnet

Then integrated over 200m, converted to a heat flux. Pre-industrial control heat budget is subtracted from the transient-future run.

Xu et al. 2022
Chang et al. 2023

Advection

diffusion + Vertical mixing

CESM-HR – advection counters warming in Indian Ocean, and western Pacific, vertical mixing counters warming in eastern Pacific

Conclusions

- Water Mass Formation
  - Spatial maps of WMF give detailed information about where deep MLD and SAMW form
  - WMF in T/S space allows us to understand the volume census and storage in SubAntarctic Zone
  - The WMF can be used quantitatively in volume budgets to identify processes of formation, destruction, & movement of water masses

- Reduced SST and upper ocean heat content warming under climate change in SubAntarctic zone in CESM-HR
  - Combination of the effects of ocean advection and also vertical mixing